Macromolecules

Article

pubs.acs.org/Macromolecules

Improved All-Polymer Solar Cell Performance of n-Type Naphthalene Diimide–Bithiophene P(NDI2OD-T2) Copolymer by Incorporation of Perylene Diimide as Coacceptor

Sandeep Sharma,[†,‡] Nagesh B. Kolhe,[†,‡] Vinay Gupta,[*,§,∥] Vishal Bharti,[‡,∥] Abhishek Sharma,[‡,∥] Ram Datt,[‡,∥] Suresh Chand,[§,∥] and S. K. Asha[*,†,‡,§]

[†]Polymer Science and Engineering Division, CSIR-National Chemical Laboratory, Pune, India 411008

[‡]Academy of Scientific and Innovative Research, New Delhi, India 110025

[§]CSIR-Network Institutes of Solar Energy, New Delhi, India

[∥]National Physical Laboratory, New Delhi, India 110012

Supporting Information

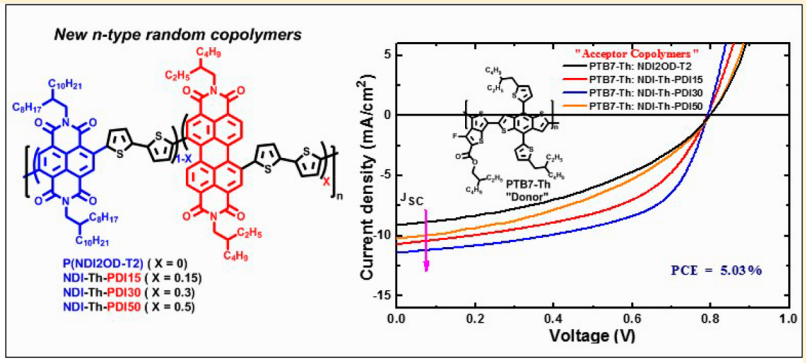

ABSTRACT: Naphthalene diimide–bithiophene P(NDI2OD-T2) is a well-known donor–acceptor polymer, previously explored as n-type material in all-polymer solar cells (all-PSCs) and organic field effect transistor (OFETs) applications. The optical, bulk, electrochemical, and semiconducting properties of P(NDI2OD-T2) polymer were tuned via random incorporation of perylene diimide (PDI) as coacceptor with naphthalene diimide (NDI). Three random copolymers containing 2,2′-bithiophene as donor unit and varying compositions of naphthalene diimide (NDI) and perylene diimide (*x*PDI, *x* = 15, 30, and 50 mol % of PDI) as two mixed acceptors were synthesized by Stille coupling copolymerization. Proton NMR spectra recorded in $CDCl_3$ showed that the $\pi-\pi$ stacking induced aggregation among the naphthalene units could be successfully disrupted by the random incorporation of bulky PDI units. The newly synthesized random copolymers were investigated as electron acceptors in BHJ all-PSCs, and their performance was compared with P(NDI2OD-T2) as reference polymer. An enhanced PCE of 5.03% was observed for BHJ all-PSCs (all-polymer solar cells) fabricated using NDI-Th-PDI30 as acceptor and PTB7-Th as donor, while the reference polymer blend with the same donor polymer exhibited PCE of 2.97% efficiency under similar conditions. SCLC bulk carrier mobility measured for blend devices showed improved charge mobility compared to reference polymer, with PTB7-Th:NDI-Th-PDI30 blend device exhibiting the high hole and electron mobility of 4.2×10^{-4} and 1.5×10^{-4} $cm^2/(V\ s)$, respectively. This work demonstrates the importance of molecular design via random copolymer strategy to control the bulk crystallinity, compatibility, blend morphology, and solar cell performance of n-type copolymers.

INTRODUCTION

The research based on solution processable organic bulk-heterojunction (BHJ) solar cells is progressing very fast. Continuous efforts have been made to increase the power conversion efficiency (PCE) of BHJ solar cell via development in both the active layer material design (n-type and p-type) and the device engineering.[1−3] In all-polymer BHJ solar cells (PSCs), both components of the active layer, i.e., electron donor and acceptor, are polymeric semiconductors which have potential advantages over the extensively studied donor polymer/acceptor fullerene composite solar cells.[4,5] Although significant progress has been made in the development of polymer/fullerene composite solar cell in terms of their high device efficiency over >9%, the use of fullerene acceptor ($PC_{61}BM$ and $PC_{71}BM$) has some disadvantages like relatively weak absorption ability in the visible region, high cost of synthesis, and morphological instability of polymer/fullerene blend over time and temperature that limits the performance of

Received: July 20, 2016
Revised: October 7, 2016
Published: October 19, 2016

DOI: 10.1021/acs.macromol.6b01566
Macromolecules 2016, 49, 8113–8125

the solar cell.[6−9] On the other hand, non-fullerene n-type polymeric acceptors have promising features such as high absorption in visible-infrared region, low cost, high thermal and photochemical stability, mechanical flexibility, and synthetic adaptability.[1,4,10,11] Among the various n-type polymeric semiconductors used in all-polymer BHJ solar cells, the polymers based on the naphthalene diimide (NDI) and perylene diimide (PDI) have exhibited the most promising features. They have high electron affinity, good absorption, thermal and photochemical stability, and π-stacking behavior which facilitates favorable solid state packing.[12−14] Particularly, the low band gap core-substituted NDI donor−acceptor polymers comprised of bithiophene and selenophene donors have attracted much attention due to their high electron mobility in OFET and high PCE efficiency in solar cells.[15−28] Poly{[*N*,*N*′-bis(2-octyldodecyl)-1,4,5,8-naphthalene-dicarboximide-2,6-diyl]-*alt*-5,5′-(2,2′-bithiophene)}, P-(NDI2OD-T2) (Polyera ActivInk N2200), is one of the extensively studied high performing n-type polymers reported by Facchetii et al.[15,27] P(NDI2OD-T2) polymer was extensively utilized in all-PSCs and OFET applications due to its desirable photophysical and semiconducting properties. It exhibited properties like high electron mobility >0.85 $cm^2\ V^{-1}\ s^{-1}$ in OFET, high PCE efficiency >5% in all-PSCs, solution processability, high crystalline nature, and light absorption capability near visible and infrared region.[15,16,20] However, it exhibited a strong tendency to form aggregates in specific organic solvents that resulted in large-scale phase separation instead of the desirable pure donor/acceptor microphase separation.[28] Consequently, the earlier reports on the all-PSC measurements of P3HT/P(NDI2OD-T2) blend showed very low device efficiency value (PCE, 0.2%).[29,30] Later studies showed that the aggregation in P(NDI2OD-T2) could be suppressed significantly in the early stage of film formation by using more polar aromatic solvents.[31] Indeed, the solar cell devices prepared from such nonaggregated solution showed improved PCE due to good intermixing of donor and acceptor components, thereby efficiently harvesting photogenerated excitons at donor−acceptor interface. Beyond the solvent induced morphological control, the structural variations also plays a vital role in improving the blend morphology, bulk crystallinity, molecular orientation, highest occupied and lowest unoccupied molecular orbital (HOMO−LUMO) energy level, and charge transport properties of polymer. For instance, Jen et al. reported the significant enhancement in the PCE up to 6.7% of P(NDI2OD-T2) polymer by substituting the bithiophene core with more electron-withdrawing fluorine (F) atom. The F-substituted P(NDI2OD-T2) polymer exhibited good bulk crystallinity with preferential face-on orientation in the BHJ blend film, thereby facilitating improved exciton generation, dissociation, and charge transport.[17] Random copolymerization is another promising design strategy utilized for synthesis of NDI-containing acceptor polymers which showed significant improvement in the PCE in all-PSCs. NDI-based random copolymers were synthesized either by varying two different donor monomers with NDI[32−34] or by varying the acceptor comonomer (such as PDI) with NDI along with a common donor co-component.[18,35,36] Recent reports on the synthesis of NDI-based random copolymers involved the use of donor monomers such as bithiophene (BT) and thiophene (T),[32] thiophene (T) and selenophene (Se),[33] and thieno[3,2-*b*]thiophene (TT) and thienylene−vinylene−thienylene (TVT).[34] Li et al. demonstrated great improvement in the PCE of P(NDI2OD-T2) polymer by modulating its crystallinity by replacing a certain amount of bithiophene (BT) units with single thiophene (T).[32] One of the compositions containing 10 mol % (PNDI-T10) showed optimal bulk crystallinity and miscibility with donor PTB7-Th, which led to PCE as high as 7.6% after solvent annealing. The use of two mixed acceptors NDI and PDI in random copolymer along with common donor also showed promising enhancement in the PCE. Particularly Jenekhe et al. demonstrated enhancement of PCE up to 6.3% in NDI-selenophene copolymer by synthesizing NDI-selenophene/PDI-selenophene random copolymers with different incorporation of PDI into copolymer backbone.[18] These NDI-selenophene/PDI-selenophene random copolymers are one of the best reported n-type copolymers which showed optimum bulk crystallinity and compatible blend morphology with donor polymer that has resulted in improved PCE in solar cell.

Most of the aforementioned reports demonstrated the importance of systematic tuning of polymer bulk crystallinity via optimizing the different comonomer compositions in random copolymers. Bulk crystallinity is one of the key factors that is responsible for bulk morphology of donor:acceptor blend in all-PSCs.[32−34] Optimum crystallinity of acceptor polymer is highly desirable to ensure proper intermixing with donor polymer in the blend to achieve good D/A microphase separation. Inspired by these strategies, we have synthesized a series of new n-type NDI-bithiophene/PDI-bithiophene random copolymers (NDI-Th-PDI*x*) by incorporating varying amounts of perylene diimide (PDI) as coacceptor along with NDI. The effect of random copolymer compositions on their energy level, optical properties, bulk crystallinity, blend morphology, charge transport, and all-PSC performance was investigated. The all-PSCs performance of the newly synthesized random copolymers was investigated in combination with PTB7 or PTB7-Th as the donor polymer. The device efficiency was compared with that of P(NDI2OD-T2) polymer as reference. The bulk charge transport properties were measured by space charge limited current (SCLC) method, the surface morphology of blends was investigated by atomic force microscopy (AFM), thin film organization using X-ray diffraction (XRD), and photoluminescence (PL) measurements.

EXPERIMENTAL SECTION

Materials. 1,4,5,8-Naphthalenetetracarboxylic dianhydride (NTCDA), 3,4,9,10-perylenetetracarboxylic dianhydride (PTCDA), 5,5′-bis(trimethylstannyl)-2,2′-bithiophene 97%, 2-octyldodecanol, 2-ethylhexylamine, and bis(triphenylphosphine)palladium(II) dichloride ($Pd(Ph_3)_2Cl_2$) were purchased from Sigma-Aldrich and used without further purification. The donor polymers PTB7 and PTB7-Th and electron transport layer PFN (poly[(9,9-bis(3′-(*N*,*N*-dimethylamino)-propyl)-2,7-fluorene)-*alt*-2,7-(9,9-dioctylfluorene)] used in all-polymer solar cell study were purchased from 1-Materials, Canada.

Measurements. ^1H NMR and ^{13}C NMR spectra were recorded using a 200 and 400 MHz Bruker NMR spectrophotometer in $CDCl_3$ containing small amounts of TMS as internal standard. Mass spectra were recorded on Voyager-De-STR MALDI-TOF (Applied Biosystems, Framingham, MA) equipped with 337 nm pulsed nitrogen laser used for desorption and ionization. The molecular weights of polymers were determined using gel permeation chromatography (GPC). GPC measurements were carried on a Thermo Quest (TQ) GPC at 25 °C using chloroform as the mobile phase. The analysis was carried out at a flow rate of 1 mL/min using a set of five μ-Styragel HT Columns (HT-2 to HT-6) and a refractive index (RI) detector. Columns were calibrated with polystyrene standards, and the

DOI: 10.1021/acs.macromol.6b01566
Macromolecules 2016, 49, 8113−8125

molecular weights are reported with respect to polystyrene. FT-IR spectra were recorded with ATR mode using Bruker α-T spectrophotometer in the range of 4000 to 400 cm^{-1}. Absorption spectra were recorded using PerkinElmer Lambda-35 UV−vis spectrophotometer. Thermogravimetric analysis (TGA) was performed using a TGA Q 5000 thermogravimetric analyzer. Samples were run from 40 to 900 °C with a heating rate of 10 °C/min under nitrogen. DSC (differential scanning colorimetry) measurements were performed on TA Q10 differential scanning calorimeter at a heating rate of 10 °C/min under a nitrogen atmosphere. The thin film X-ray diffraction data were recorded using a Rigaku model Dmax-2500 diffractometer using Cu Kα (1.54 Å) emission, and the spectra were recorded in the range of (2θ) 2°−50°. Electrochemical behavior of NDI polymers was analyzed by cyclic voltammetry by using BAS-Epsilon potentiostat. The surface morphology of active layers of actual bulk-heterojunction (BHJ) solar cells was characterized by AFM imaging technique using the Agilent 5500 AM scanning probe microscopy in tapping mode using Si probe. PL Measurements were carried out on a PTi quanta Master-400 florescence spectrometer.

Sample Preparation. For the UV−vis absorption studies, thin films were prepared by dissolving polymer in chloroform (10 mg/mL) and spin-coating (600 rpm/60 s) on quartz plates. For the XRD analysis, films were prepared by drop-casting the highly concentrated (20 mg/mL) polymer solution in chloroform on glass slide followed by thermal annealing at 160 °C for 10 min. Thin film samples of the blend donor:acceptor polymers for PL and XRD measurements were prepared by mixing the donor PTB7-Th and acceptors P(NDI2OD-T2)/NDI-Th-PDIx in 1.3:1 (w/w) ratio in chloroform under similar conditions as that for the photovoltaic device fabrication.

Fabrication and Characterization of the Photovoltaic Cells. PTB7 or PTB7-Th as donor and P(NDI2OD-T2) and NDI-Th-PDIx (x = 15, 20, and 30 mol % of PDI) acceptors were used. PTB7 or PTB7-Th was blended with each of the four acceptors separately in chloroform and stirred at 40 °C for more than 24 h in a glovebox. The optimized donor:acceptor (D:A) ratio was 1.3:1 (w/w), and total concentration of (D + A) in chloroform solution was ∼12 mg/mL. The optimized volume fraction of 1,8-diiodooctane (DIO) additives to (D + A) in chloroform solution was 1.25 vol %. PFN (2 mg/mL) was prepared in methanol in the presence of a small amount of acetic acid (2 μL mL^{-1}). Preparation of ZnO sol−gel was done as follows. Zinc acetate dihydrate [$Zn(CH_3COO)\cdot 2H_2O$] (Aldrich, 99.9%) with 0.1 M concentration was first dissolved in anhydrous ethanol [CH_3CH_2OH] (99.5+%, Aldrich) and rigorously stirred for 2−3 h at 80 °C. Subsequently, ethanolamine was added to the solution as sol stabilizer followed by thorough mixing process with a magnetic stirrer for 12−15 h at 60 °C. Inverted type all-polymer solar cells were fabricated using an indium tin oxide (ITO)/ZnO/PFN/active layer/MoOx/Al structure. ITO-coated glass substrates were subjected to ultrasonication in soap, deionized water, acetone, and isopropyl alcohol. The substrates were then dried for several hours in an oven at 120 °C. The ITO substrates were treated with UV-ozone before ZnO sol−gel was spin-coated on the ITO-coated glass substrate with 3000 rpm for 60 s. The ZnO films were annealed at 200 °C for 1 h in the air. The thickness of ZnO film was approximately 30 nm, as determined by a profilometer. PFN was spin-coated on ITO at 2000 rpm for 60 s and baking for 15 min at 80 °C in a N_2 glovebox. Then, each active blending solution was spin-casted onto an ITO/ZnO/PFN substrate at 2000 rpm for 120 s. The final thickness of each films was 100−110 nm. Then, MoO_3 (∼10 nm) was thermally deposited in high vacuum (∼8 × 10^{-7} Torr). Finally Al (∼100 nm) was deposited in same high vacuum (∼8 × 10^{-7} Torr) over the MoO_x through the shadow mask. The active area of the devices was 10 mm^2 in all the cases.

The photovoltaic performance of the devices was characterized using a solar simulator (SCIENCTECH SS150 solar simulators) with an air-mass (AM) 1.5G filter. The intensity of the solar simulator was carefully calibrated using an AIST-certified silicon photodiode. The current−voltage behavior was measured using a Keithley 2400 SMU. EQE spectra of fabricated devices were measured using a Keithley 2600 source meter and a CEP-25 ML spectral response measurement system which shines light with AM1.5G spectral distribution and calibrated using an AIST-certified silicon photodiode to an intensity of 1000 W/m^2.

SCLC Measurement. The hole and electron mobilities of all-polymer blends and polymer neat films were measured by the space-charge-limited current (SCLC) method using hole only configuration ITO/MoOx (10 nm)/active layer (∼100 nm)/Au (200 nm) structure and electron only configuration ITO/ZnO (30 nm)/active layer (∼100 nm)//Al (100 nm). In both the cases, active layer was spin-casted exactly the same way as it was done in the case of photovoltaic cells discussed above. Current−voltage measurements in the range of 0−10 V were taken, and the results were fitted to a space-charge-limited function with active area of the devices as 10 mm^2. The carrier mobility was extracted by fitting the J−V curves in the near quadratic region according to the modified Mott−Gurney equation:[37]

$$J(V) := \frac{9}{8}\varepsilon\mu\left(\frac{V^2}{L^3}\right)e^{0.89\beta\sqrt{V/L}}$$

where J is the current density, $\varepsilon = \varepsilon_0\cdot\varepsilon_r$, ε_0 (8.85 × 10^{14} F/cm) is the permittivity of free space, ε_r is the dielectric constant of the organic semiconductor (assumed to be 3.2), μ is the zero-field mobility, V is the applied voltage, L is the thickness of active layer, and β is the field-activation factor. The current−voltage curves and SCLC fittings of the data are shown in Supporting Information Figure 16, and the bulk carrier mobilities are summarized in Table 4.

Synthesis of Homo and Random Copolymers. *Poly{[N,N′-bis(2-octyldodecyl)-1,4,5,8-naphthalenedicarboximide-2,6-diyl]-alt-5,5′-(2,2′-bithiophene)}, P(NDI2OD-T2).* NDI-2OD-Br2 (0.4 g, 0.406 mmol) and 5,5′-bis(trimethylstannyl)-2,2′-bithiophene (0.199 g, 0.406 mmol) were taken in an air-free Schlenk tube under N_2 atmosphere. Dry toluene (18 mL) was added in the tube followed by purging with nitrogen for half-hour. Bis(triphenylphosphine)palladium(II) dichloride ($Pd(Ph_3)_2Cl_2$) (15 mg, 0.0211 mmol) was added to the tube quickly by opening rubber septa, and the whole mixture was degassed by four freeze−vacuum−thaw cycles. The reaction mixture was stirred at 90−95 °C for 3 days. Bromobenzene (0.2 mL) was then added, and the reaction mixture was further stirred at 90−95 °C for 12 h. Upon cooling to room temperature, a solution of potassium fluoride (1 g) in 2 mL of water was added and stirred for 2 h. The reaction mixture was extracted with chloroform (250 mL × 3). The organic layer was washed with water, dried over anhydrous sodium sulfate, and concentrated on a rotary evaporator. The obtained residue was dried in a vacuum oven and subjected to a Soxhlet extraction with acetone (48 h) and chloroform (12 h). Half of the chloroform was evaporated on rota, and the remaining chloroform solution containing polymer was precipitated in 500 mL of methanol, stirred for 2 h, filtered on a Buchner funnel, washed with plenty of methanol, and dried in vacuum. The polymer was obtained as a deep blue solid. Yield 0.380 g (95%). ^{1}H NMR (400 MHz, $CDCl_3$) δ ppm: 8.82−8.5 (br, 2H),7.33 (br, 4H), 4.11 (br, 4H), 1.98 (br, 2H), 1.24 (br, 64H), 0.84 (br, 12 H). (FTIR ATR, cm^{-1}): 2919, 2923, 2857, 1699, 1658, 1586, 1501, 1432, 1386, 1325, 1232, 1181, 1146, 1094, 857, 808, 739, 678. GPC: M_n, 26.4 kDa; M_w, 152 kDa; M_w/M_n, 5.7.

Poly{([N,N′-bis(2-octyldodecyl)naphthalene-1,4,5,8-bis-(dicarboximide)-2,6-diyl]-alt-5,5′-2,2′-bithiophene)-ran-([N,N′-bis-(2-ethylhexyl)-1,7-dibromo-3,4,9,10-perylenediimide]-alt-5,5′-2,2′-bithiophene)}. All the random copolymers, i.e., NDI-Th-PDI15, NDI-Th-PDI30, and NDI-Th-PDI50, were synthesized using same procedure as that given for P(NDI2OD-T2), but with different mole ratios of NDI-2OD-Br2 to PDI-2OD-Br2.

NDI-Th-PDI15. NDI-Th-PDI15 was synthesized using 0.199 g (0.406 mmol) of 5,5′-bis(trimethylstannyl)-2,2′-bithiophene, 0.340 g (0.345 mmol) of NDI-2OD-Br2, 47 mg (0.0609 mmol) of PDI-2EH-Br2, and 15 mg (0.0211 mmol) of $Pd(Ph_3)_2Cl_2$. Yield: 0.360 g (86%). ^{1}H NMR (400 MHz, $CDCl_3$) δ ppm: 8.81, 8.5 (br, 2H naphthalene aromatic), 8.73 (br, 2H perylene aromatic), 8.37 (br, 4H perylene aromatic), 7.33 (br, 4H bithiophene), 4.10 (br, 8H), 1.97 (br, 4H), 1.24 (br, 80H), 0.84 (br, 24 H). FTIR (ATR, cm^{-1}): 2919, 2851, 1703, 1662, 1571, 1574, 1433, 1377, 1305, 1243, 1188, 1053, 965, 928, 787, 717. GPC: M_n, 16.4 kDa; M_w, 60.7 kDa; M_w/M_n, 3.7.

DOI: 10.1021/acs.macromol.6b01566
Macromolecules 2016, 49, 8113−8125

Scheme 1. Chemical Structures of P(NDI2OD-T2) Acceptor and PTB7/PTB7-Th Donor Polymers

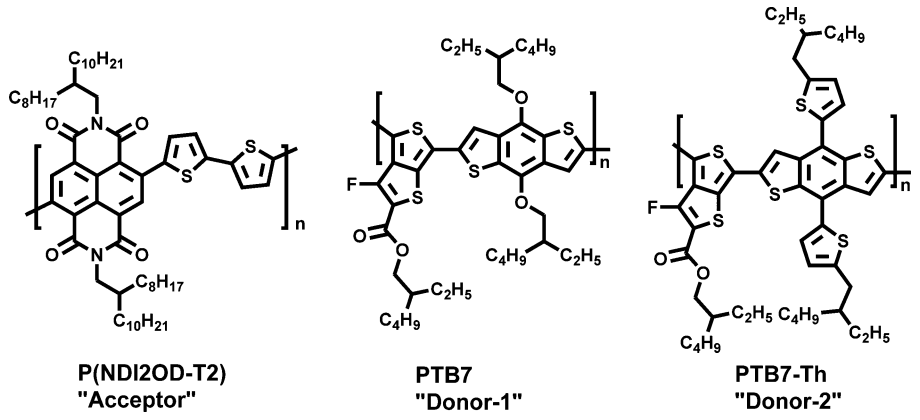

NDI-Th-PDI30. NDI-Th-PDI30 was synthesized using 0.250 g (0.508 mmol) of 5,5′-bis(trimethylstannyl)-2,2′-bithiophene, 0.350 g (0.355 mmol) of NDI-2OD-Br2, 117 mg (0.152 mmol) of PDI-2EH-Br2, and 18 mg (0.0264 mmol) of $Pd(Ph_3)_2Cl_2$. Yield: 0.450 g (88%). ^{1}H NMR (400 MHz, $CDCl_3$) δ ppm: 8.81 (br, 2H naphthalene aromatic), 8.71, 8.5 (br, 2H perylene aromatic), 8.36 (br, 4H perylene aromatic), 7.31 (br, 4H bithiophene), 4.11 (br, 8H), 1.97 (br, 4H), 1.23 (br, 80H), 0.84 (br, 24 H). FTIR (ATR, cm^{-1}): 2919, 2852, 1702, 1660, 1572, 1513, 1433, 1401, 1306, 1243, 1186, 1174, 1043, 963, 927, 881, 853, 768, 713, 670. GPC: M_n, 16.8 kDa; M_w, 49.8 kDa; M_w/M_n, 2.9.

NDI-Th-PDI50. NDI-Th-PDI50 was synthesized using 0.250 g (0.508 mmol) of 5,5′-bis(trimethylstannyl)-2,2′-bithiophene, 0.250 g (0.254 mmol) of NDI-2OD-Br2, 0.197 g (0.254 mmol) of PDI-2EH-Br2, and 18 mg (0.0264 mmol) of $Pd(Ph_3)_2Cl_2$. ^{1}H NMR (400 MHz, $CDCl_3$) δ ppm: 8.79 (br, 2H naphthalene aromatic), 8.69 (br, 2H perylene aromatic), 8.35 (br, 4H perylene aromatic), 7.33 (br, 4H bithiophene), 4.11 (br, 8H), 1.96 (br, 4H), 1.21 (br, 80H), 0.81 (br, 24 H). FTIR (ATR, cm^{-1}): 2921, 2852, 1700, 1660, 1587, 1433, 1401, 1374, 1313, 1244, 1188, 1036, 860, 712, 755, 715, 761. GPC: M_n, 12.6 kDa; M_w, 32.4 kDa; M_w/M_n, 2.5.

RESULTS AND DISCUSSION

Synthesis and Characterization. Poly{[*N*,*N*′-bis(2-octyldodecyl)-1,4,5,8-naphthalenedicarboximide-2,6-diyl]-*alt*-5,5′-(2,2′-bithiophene)} P(NDI2OD-T2) and its random copolymers NDI bithiophene/PDI bithiophene incorporating various mole percentages of perylene diimide (PDI) were synthesized by Stille coupling polymerization. The molecular structure of P(NDI2OD-T2) is depicted in Scheme 1, and the synthesis of random copolymers is outlined in Scheme 2. The synthesis of monomers *N*,*N*′-bis(2-octyldodecyl)-2,6-dibromonaphthalene-1,4:5,8-tetracarboxylic diimide (NDI-2OD-Br2) and *N*,*N*′-bis(2-ethylhexyl)-1,7-dibromo-3,4,9,10-perylenetetracarboxylic diimide (PDI-2EH-Br2) were carried out according to previously reported procedures (Supporting Information).[38−40] Elemental analysis of the monomers was carried out to confirm the purity, and the observed CHN values were matching with the calculated values which are given in the Supporting Information. The monomers were subsequently subjected to MALDI-TOF analysis recorded using 2,5-dihydroxybenzoic acid as the matrix, and molecular ion peaks were obtained for cationic species such as [M + 1] and [M + Na^+]. The MALDI spectra of the monomers are given in the Supporting Information (Figure S1). Three random copolymers, i.e., NDI-Th-PDI15, NDI-Th-PDI30, and NDI-Th-PDI50, were synthesized by varying the feed ratio of the two monomers NDI-2OD-Br2 and PDI-2EH-Br2 (15, 30, and 50 mol % of PDI) while maintaining the concentration of the donor bithiophene comonomer constant (1 mol) in feed. The higher incorporation of PDI-2EH-Br2 monomer having short alkyl side chain (2-ethylhexyl) produced random copolymers which had limited solubility in common organic solvents. The maximum incorporation of 50 mol % of PDI in random copolymer (NDI-Th-PDI50) was found to retain good solubility in common organic solvents like chloroform, chlorobenzene, and dichlorobenzene, etc. The alternate copolymer NDI-bithiophene (P(NDI2OD-T2), Scheme 1) was also synthesized as a reference benchmark. The structures of monomers and polymers were characterized by ^{1}H NMR, ^{13}C NMR, and FTIR spectra. The NMR and MALDI-TOF spectra and elemental analysis of the molecules confirmed the structure and high purity of the monomers.

Scheme 2. Synthesis of n-Type NDI-Bithiophene/PDI-Bithiophene Random Copolymers

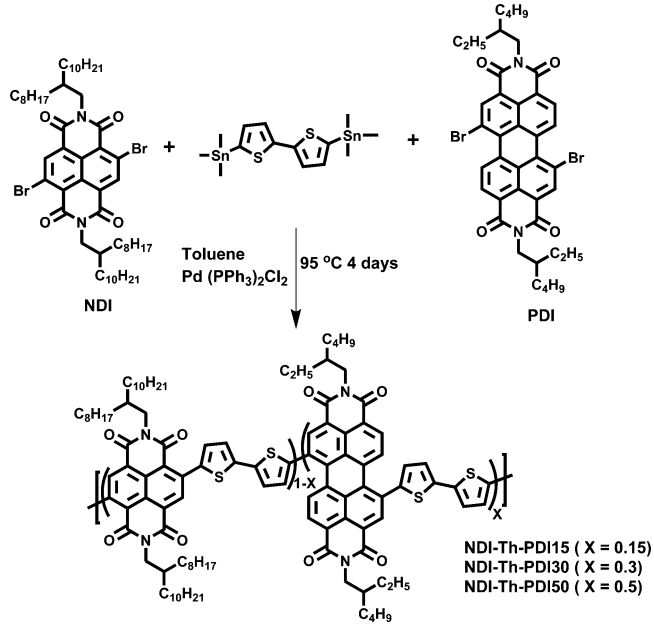

The labeled ^{1}H NMR spectra of monomer (NDI-2OD-Br2 and PDI-2EH-Br2) and copolymers are given in the Supporting Information (Figures S2−S7). The actual incorporation of the PDI in the random copolymers could be determined from the proton NMR spectra. Figure 1 shows the expanded aromatic region (6.0−9.5 ppm) in the proton NMR spectra of the

DOI: 10.1021/acs.macromol.6b01566
Macromolecules 2016, 49, 8113−8125

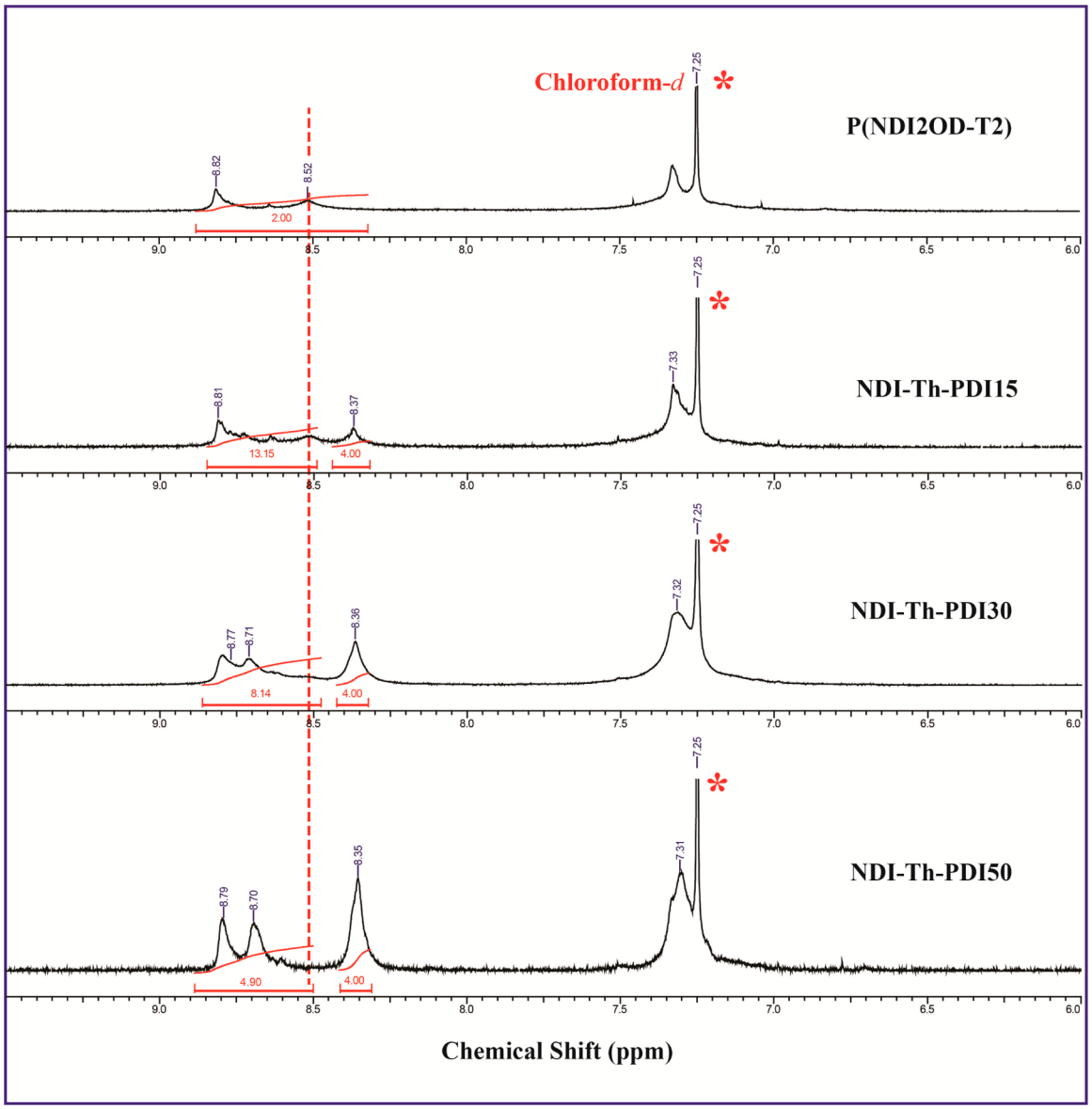

Figure 1. ^{1}H NMR spectra of copolymers (expanded aromatic region) recorded in $CDCl_3$.

Table 1. GPC Molecular Weight and Thermal Characteristics of P(NDI2OD-T2) and NDI-Th-PDI*x* Random Copolymers

polymer	M_w[a] (kDa)	M_w/M_n[b]	T_d[c] (°C)	T_m[d] (°C)	ΔH_m[d] (J/g)	$\Delta H_{m,blend}$[e] (J/g)
P(NDI2OD-T2)	152	5.7	422	286.61	6.65	2.56
NDI-Th-PDI15	60.7	3.7	437	289.47	12.57	1.77
NDI-Th-PDI30	49.8	2.9	435	284.0	6.55	1.49
NDI-Th-PDI50	32.4	2.5	436	269.38	4.41	

[a]Weight-average molecular weight (M_w). [b]Polydispersity index (M_w/M_n). [c]The decomposition temperature (5% weight loss) estimated using TGA under N_2. [d]Measured using DSC under N_2. [e]Enthalpy for blend PTb7-Th: P(NDI2OD-T2) and PTB7-Th:NDI-Th-PDI*x* (1.3:1, w/w).

reference and random copolymers. The ^{1}H NMR spectra of reference polymer P(NDI2OD-T2) exhibited one extra broad peak at ~8.5 ppm which has been attributed to strong interchain aggregation of P(NDI2OD-T2) in chloroform.[28,29,41] The peaks at 8.5 and 8.82 ppm together accounted for the two aromatic protons of naphthalene core, while the peak at 7.33 ppm corresponded to the four protons of the bithiophene unit. From the figure it could be seen that in the random copolymers the extra peak for aggregation diminished progressively with the incorporation of PDI units and two new peaks at ~8.35 ppm (four protons) and ~8.70 (two protons) ppm appeared for PDI aromatic protons, whose intensity increased progressively. The dotted line in Figure 1 indicates the position of the aggregated naphthyl aromatic protons. The peak at 8.70 ppm for two aromatic protons of PDI overlapped with the aromatic protons of NDI. However, knowing the contribution of single PDI proton from the PDI proton integration at 8.35 ppm, the value could be subtracted from the integration in the 8.5−8.8 ppm region. Thus, the PDI incorporation was calculated as 15, 29, and 43% respectively

DOI: 10.1021/acs.macromol.6b01566
Macromolecules 2016, 49, 8113−8125

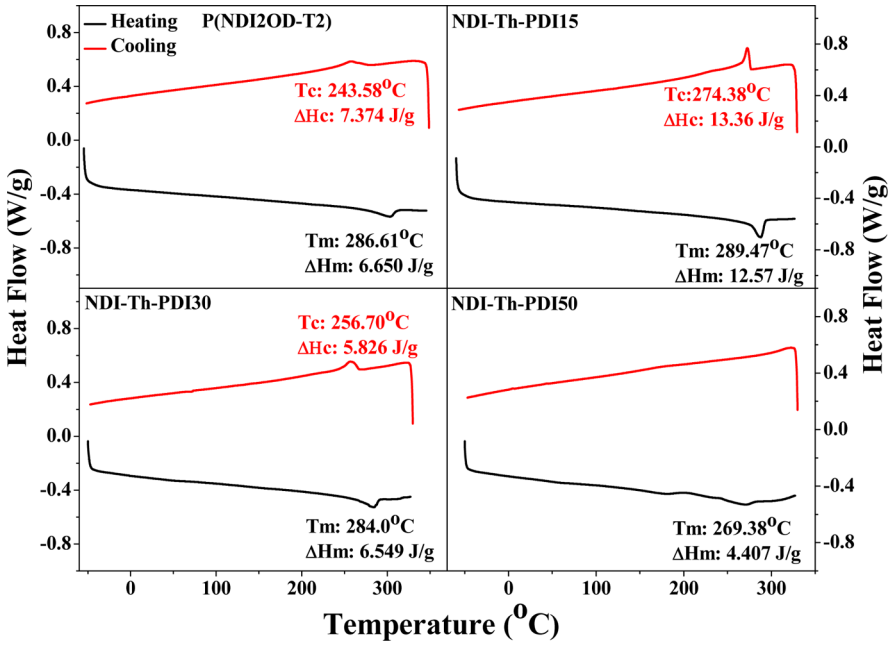

Figure 2. Second heating/cooling curves of quench−cooled samples of the copolymers in the DSC scans conducted at 10 °C/min under a N_2 atmosphere.

for the three copolymers having 15, 30, and 50 mol % of PDI in the feed. For the sake of simplicity, the polymers were labeled as NDI-Th-PDI15, NDI-Th-PDI30, and NDI-Th-PDI50 even though the actual incorporation was slightly different.

The reference as well as newly synthesized random copolymers showed good solubility in common organic solvents like chloroform, chlorobenzene, and dichlorobenzene, etc., and their molecular weights were determined by gel permeation chromatography (GPC), using polystyrene standards for the calibration with chloroform as solvent. The GPC traces are shown in Figure S8. The benchmark copolymer P(NDI2OD-T2) showed weight-average molecular weight (M_w) of 152 kDa with M_w/M_n of 5.7. These values are comparable with literature reports.[27,28] Random copolymers showed lower weight-average molecular weight (M_w) and M_w/M_n with M_w in the range of 32.4−60.7 kDa and PDI in range of 2.5−3.1 (Table 1). Furthermore, the M_w and M_w/M_n were found to decrease as the content of PDI unit increased in the random copolymer. The lower value of M_w and M_w/M_n in random copolymers indicated their less interchain aggregation in chloroform compared to the reference polymer P-(NDI2ODT2). The reduced solubility of the PDI comonomer having short alkyl side chain (2-ethylhexyl) could also be a reason for the decrease in molecular weights in copolymers with higher PDI incorporation. The thermal properties of the copolymers were determined by thermogravimetric analysis (TGA) as well as differential scanning calorimetry (DSC) measured under a nitrogen atmosphere. TGA curves (given in Figure S9) showed good thermal stability for all random copolymers with onset decomposition temperature (T_d) of over >400 °C. Literature cites a melting transition for P(NDI2OD-T2) with onset around 280 °C (heating scan), indicating the crystalline nature of the polymer.[15,42] DSC curves were recorded for all polymers by heating from −50 °C until 330 °C at 10 °C/min under N_2 atmosphere. P(NDI2OD-T2) showed a broad thermal transition with endothermic peak (T_m) at 287 °C and exothermic peak at (T_c) 244 °C with melting and cooling enthalpy values (ΔH_m) 6.65 J/g and (ΔH_c) 7.37 J/g, respectively. NDI-Th-PDI15 and NDI-Th-PDI30 also showed the melting and crystallization transitions in their second heating and cooling cycles. However, NDI-Th-PDI50 did not exhibit a reversible thermal transition in the cooling cycle, but a transition was observed in the first and second heating cycles. In order to compare the relative crystallinity of the polymers based on the enthalpies of transition, a quench-cooling experiment was carried out to obtain perfectly reproducible thermograms. Essentially, this experiment involved heating carefully weighed samples (5−6 mg) of the polymer in a crimped DSC pan from room temperature (25 °C) to 330 °C to melt them and then immediately quenching the DSC sample pan using liquid nitrogen. The sample pan was then later heated from −50 to 330 °C and then again cooled back to −50 °C. This procedure enables to cool and equilibrate quickly in order to detect the complete crystallization during the next heating cycle. Figure 2 gives the heating and cooling scans collected for all the four polymers after the quenching experiment. Table 1 lists the melting temperature (T_m) and corresponding enthalpies (ΔH_m) obtained for the four polymers. NDI-Th-PDI15 showed a much sharper melting and crystallization transitions with almost double the value for enthalpy compared to P(NDI2OD-T2). Its transition temperatures were also slightly higher compared to the reference polymer. NDI-Th-PDI30 had almost similar transition temperature and enthalpy values compared to the reference polymer. For the reference as well as NDI-Th-PDI15 and NDI-Th-PDI30 polymers very good reversibility was observed for the endo- as well as exothermic transitions. However, NDI-Th-PDI50 showed a broad endothermic transition at 269 °C, which was much low compared to the reference polymer (286.9 °C), and no exothermic transition was observed during the cooling cycle.

The enthalpy of melting (ΔH_m) obtained from the area of melting transition could be correlated to the crystallinity.[32,43] The comparison of ΔH_m showed that NDI-Th-PDI15 exhibited

DOI: 10.1021/acs.macromol.6b01566
Macromolecules 2016, 49, 8113−8125

relatively higher crystallinity (ΔH_m, 12.57 J/g) compared to the reference polymer P(NDI2OD-T2) (ΔH_m, 6.65 J/g), while NDI-Th-PDI30 (ΔH_m, 6.45 J/g) had slightly lower and NDI-Th-PDI50 (ΔH_m, 4.41 J/g) had the lowest crystallinity. The observation from DSC suggested that low incorporation of PDI (<15 mol %) did not disrupt the packing of the polymer chain backbone, whereas >30 mol % of PDI in the backbone disrupted the chain packing leading to sluggishness in crystallization. Furthermore, the reduction in crystallinity of NDI-Th-PDI30 and NDI-Th-PDI50 with high PDI incorporation supported the observation from the proton NMR spectra of reduced NDI stacking with increased PDI content.

Optical and Electrochemical Properties. UV−vis absorption spectra of random copolymers (NDI-Th-PDI*x*) and reference P(NDI2OD-T2) were recorded in both dilute chloroform solution and thin film spin-coated on glass substrate and are shown in Figure 3. In solution (top) all copolymers showed two distict absorption bands; the first high energy absorption band at ∼300−425 nm was accounted for by $\pi-\pi^*$ transition, and another low energy band at ∼460−800 nm was assigned to intramolecular charge transfer (ICT) from bithiophene unit to NDI/PDI.[28] The reference polymer P(NDI2OD-T2) showed typical absorption spectrum with $\pi-\pi^*$ absorption peak at ∼400 nm and ICT peak at 645 nm. In the random copolymers the position of the $\pi-\pi^*$ absorption peak remained unchanged, while the ICT absorption band was found to be blue-shifted (hypsochromic shift). It was observed at 630 nm in NDI-Th-PDI15, 618 nm in NDI-Th-PDI30, and 605 nm in NDI-Th-PDI50. The progressive hypsochromic shift observed in ICT absorption band of random copolymers could be accounted for by the reduced planarity of the polymer backbone when compared to P(NDI2OD-T2). The reference polymer P(NDI2OD-T2) is well-known to form self-aggregates in chloroform due to strong interchain stacking of more planar polymer backbone, which leads to a red-shifted ICT band.[28] Incorporation of the large PDI units in the random copolymers reduced the planarity of the polymer backbone as well as interchain aggregation.[35] Consequently, the ICT band was shifted to lower wavelength. Furthermore, an additional broad peak at ∼500 nm was obtained for all random copolymers which was absent in P(NDI2OD-T2), and the intensity of this peak at ∼500 nm was found to increase with the increase in the content of PDI unit. This additional peak was assigned for the typical absorption of the PDI component in the random copolymer. The spin-coated thin films of all copolymers showed similar absorption spectra as that in solution (Figure 3, bottom), except for the large red-shifting of the ICT band in the solid state compared to that in solution due to the interchain aggregation and chain planarization.[35] The reference copolymer P(NDI2OD-T2) showed ICT band at 685 nm. On the other hand, random copolymers NDI-Th-PDI15, NDI-Th-PDI30, and NDI-Th-PDI50 exhibited blue-shifted ICT band along with decreased absorption coefficient at 670, 655, and 630 nm, respectively. The large blue-shifting of ICT band in random copolymer indicated less interchain stacking and aggregation in solid state compared to P(NDI2OD-T2). The reduced self-aggregation of random copolymer could be beneficial to improve the intermixing of n-type random copolymer with donor polymer to form compatible blend which is discussed later on in the all-PSCs device section. The optical band gaps (E_g^{opt}) of random copolymers were calculated from lower energy absorption band edge of thin film and are listed in Table 2. An optical band gap of 1.52 eV was obtained for reference copolymer P(NDI2OD-T2) which was slightly increased to 1.55, 1.57, and 1.60 eV in NDI-Th-PDI15, NDI-Th-PDI30, and NDI-Th-PDI50, respectively. Electrochemical redox behavior and electronic energy levels of new n-type random copolymers were analyzed by cyclic voltammetry. Thin films of polymer were deposited on the platinum working electrode. The measurement was carried out in acetonitrile solvent with ferrocene/ferrocenium as an internal standard and tetrabutylammonium hexafluorophosphate (n-Bu_4NPF_6 0.1 M/

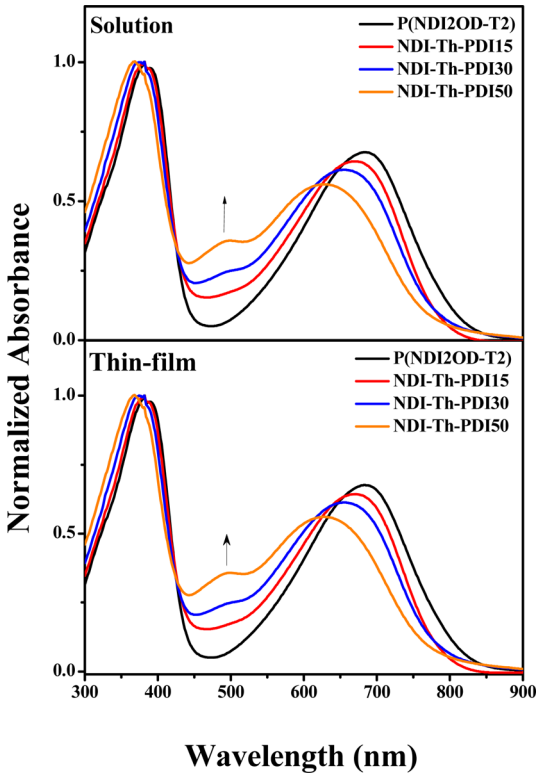

Figure 3. UV−vis absorption spectra of dilute solutions of reference P(NDI2OD-T2) and random copolymers in chloroform (top) and thin film (bottom) on glass substrate.

Table 2. UV−Vis Absorption, Optical Band Gap, Electronic Energy Levels, and Thin-Film XRD Data of Thermally Annealed Random Copolymers of P(NDI2OD-T2) and NDI-Th-PDI*x* Random Copolymers

	λ_{max} (nm)					2θ (deg)		d-spacing (Å)	
polymer	solution	thin film	E_g^{opt} (eV)	LUMO (eV)	HOMO (eV)	(100)	(010)	d_{100}	d_{010}
P(NDI2OD-T2)	367, 645	381, 685	1.52	3.90	5.42	4.06	23.10	21.72	3.84
NDI-Th-PDI15	367, 630	381, 670	1.55	3.94	5.49	4.21	23.03	20.96	3.85
NDI-Th-PDI30	367, 618	374, 655	1.57	3.94	5.51	4.58	22.59	19.27	3.93
NDI-Th-PDI50	367, 605	368, 630	1.60	4.00	5.60	4.80	21.92	18.38	4.00

DOI: 10.1021/acs.macromol.6b01566
Macromolecules 2016, 49, 8113−8125

acetonitrile) as supporting electrolyte.[44] Cyclic voltammograms for all copolymers are shown in Figure S10, and the calculated HOMO and LUMO energy levels are given in Table 2. Thin film of reference polymer P(NDI2OD-T2) exhibited two reversible reduction peaks, which were attributed to the formation of radical anion and dianions of NDI in the polymer backbone.[27]All random copolymers showed quasi-reversible reduction peaks with almost similar values of electrochemical reduction like P(NDI2OD-T2). None of the copolymer showed oxidation peak during anodic scan up to 2 V. The lowest occupied molecular orbital (LUMO) energy levels were estimated based on the onset value of first reduction peak and reference energy level of ferrocene (4.8 eV below the vacuum level) according to E_{LUMO} (eV) = $-e \times (E^{red}_{onset} + 4.8)$ below the vacuum level.[44] The highest occupied molecular orbital (HOMO) levels were calculated based on the optical band gap obtained from the solid state absorption onset measurements. The LUMO and HOMO energy levels of P(NDI2OD-T2) were found to be −3.90 eV and −5.42 eV, respectively, which resemble the previously reported values.[27,44] Newly synthesized random copolymers exhibited almost similar values for energy level (LUMO and HOMO) (Table 2) like reference polymer P(NDI2OD-T2). This suggested that there was a negligible effect of incorporation of PDI unit on the energy level of random copolymers, and both the components NDI and PDI exhibited almost similar electron accepting strength.

Thin-Film Crystallinity. The molecular packing and bulk crystalline nature of reference P(NDI2OD-T2) and new n-type random copolymers were analyzed using wide-angle X-ray diffraction (XRD) measurement. Figure 4 shows the X-ray diffraction patterns of thermally annealed (at 160 °C, 10 min) thin films of copolymer on glass substrate, and relevant data are given in Table 2. The XRD pattern of reference polymer P(NDI2OD-T2) showed lamellar peak (100) at 2θ = 4.06° and $\pi-\pi$ stacking peak (010) at 2θ = 23.10°, which corresponded to lamellar packing distance of 21.72 Å and $\pi-\pi$ stacking distance of 3.84 Å. The lamellar peak (100) for random copolymers was observed at 2θ = 4.21°, 4.58°, and 4.80° with *d*-spacing 20.96, 19.27, and 18.38 Å for NDI-Th-PDI15, NDI-Th-PDI30, and NDI-Th-PDI50, respectively. The lamellar packing distance was found to decrease progressively with increasing incorporation of PDI moiety in the random copolymer chain. This observation is very similar to the previous results by Jenekhe et al. and could be attributed to the shorter 2-ethylhexyl side chains on PDI moiety.[18] In contrast, the $\pi-\pi$ stacking distance increased linearly with increasing incorporation of PDI moiety into the copolymer chain (Figure 4, inset). It increased from 3.84 Å in reference P(NDI2OD-T2) to 3.85, 3.93, and 4.00 Å in NDI-Th-PDI15, NDI-Th-PDI30, and NDI-Th-PDI50, respectively. Overall, all the random copolymers (NDI-Th-PDI*x*) exhibited sharp and intense peaks with the lamellar ordering observed up to third order in XRD (Figure S11), indicating their highly crystalline nature.

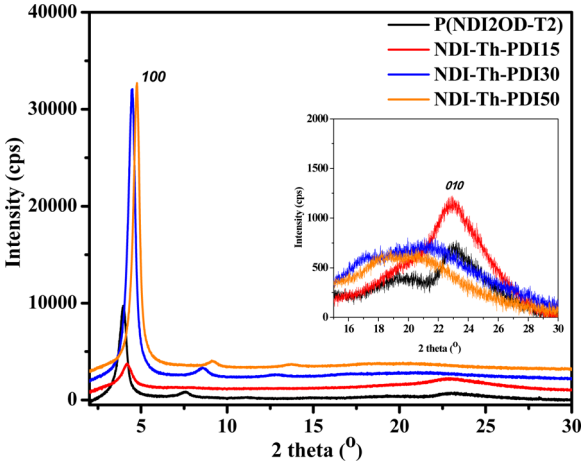

Figure 4. Thin-film XRD diffraction patterns of reference P(NDI2OD-T2) and random copolymers.

D:A Blend Property Analysis. It is important to study the behavior of the donor:acceptor copolymer blend in order to understand their photovoltaic device performance. Therefore, blend samples were prepared by mixing donor:acceptor (D:A) in the ratio 1.3:1 (w/w) choosing PTB7-Th as the standard donor polymer which produced relatively higher PCE. This D:A blend ratio (1.3:1) was found to be optimum for all-PSCs which is described later on. The thermal analysis of the blend samples were performed using DSC under identical quench−cooling conditions as was employed for the pristine samples. The thermograms of the blends of the reference as well as PDI copolymers are given in Figure S12, and the values of the melting transition enthalpies (ΔH_m) are listed in Table 1. The donor PTB7-Th did not exhibit a melting transition under similar conditions. All blend samples exhibited reduction in the enthalpy of melting (2.56, 1.77, and 1.49 J/g for P(NDI2OD-T2), NDI-Th-PDI15, and NDI-Th-PDI30, respectively) compared to the pristine samples (6.65, 12.57, and 6.55 J/g, respectively). The NDI-Th-PDI50 copolymer blend did not exhibit any transition even after being subjected to the quench−cooling procedure. The reduced crystallinity indicated better donor:acceptor miscibility in the blend.

The thin films of the blends were next analyzed using wide-angle X-ray diffraction studies, and the corresponding diffraction patterns are shown in Figure S13. It was observed that the sharp and intense peaks for the lamellar ordering observed in the pristine samples (Figure S11) were mostly retained in the blends of PTB7-Th with P(NDI2OD-T2) and NDI-Th-PDI15 (indicated by arrow in the Figure S13). It could be seen that the reference blend PTB7-Th:P(NDI2OD-T2) exhibited relatively more number of peaks compared to the random copolymers, which suggested that it did not form good compatible blends. The higher ordered lamellar peaks were mostly not observed in the blends of NDI-Th-PDI30 and NDI-Th-PDI50. The (100) and the $\pi-\pi$ stacking peak were the only prominent peaks in these blends. The absence of higher ordered lamellar peaks indicated that the copolymers with higher PDI content like the NDI-Th-PDI30 and NDI-Th-PDI50 formed more compatible donor−acceptor blends.

The PTB7-Th:acceptor blend films were further analyzed by photoluminescence (PL) quenching experiments to investigate the exciton diffusion and dissociation. Figure S14 shows the steady-state PL spectra of the neat PTB7-Th, P(NDI2OD-T2), NDI-Th-PDI15, NDI-Th-PDI30, and NDI-Th-PDI50 along with their blend films with PTB7-Th. The PL spectra (at excitation wavelength 645 nm)[32] of neat PTB7-Th showed peak maxima at ∼755 nm, while acceptor polymers exhibited broad peaks in the range of ∼800−830 nm. All D/A blend films showed significant PL quenching compared to neat PTB7-Th. The relative PL quenching efficiency (ΔPL) was estimated by measuring the intensity of various D/A blend with respect to neat PTB7-Th (Figure S15).[32] The PTB7-Th:P(NDI2OD-T2)

DOI: 10.1021/acs.macromol.6b01566
Macromolecules 2016, 49, 8113−8125

reference blend showed ΔPL ~ 76%, while PTB7-Th:NDI-Th-PDI15, PTB7-Th:NDI-Th-PDI30, and PTB7-Th:NDI-Th-PDI50 exhibited ΔPL of ~86%, ~87%, and ~91%, respectively. Higher ΔPL in the random copolymer blends indicated efficient exciton dissociation at D/A interface as a result of good intermixing of acceptor polymer with PTB7-Th. Overall, the thermal property, crystallinity, and PL quenching efficiency of the blends pointed toward the copolymers' ability to perform better in photovoltaic devices compared to the reference polymer, especially for the copolymers with higher PDI content, i.e., PTB7-Th:NDI-Th-PDI30 and PTB7-Th:NDI-Th-PDI50.

All-Polymer BHJ Solar Cells. The potential application of random copolymers (NDI-Th-PDI*x*) as acceptor (n-type) materials in all-polymer solar cells was explored by fabricating BHJ all-PSCs using PTB7 or PTB7-Th polymers as electron donor materials. The inverted devices with configuration of ITO/ZnO/PFN/polymer blend/Al were fabricated. The detailed procedure for device structure and fabrication is given in the Experimental Section. The all-PSCs device using n-type reference polymer P(NDI2OD-T2) was also fabricated for comparison. The blend active layers of donor:acceptor polymers were deposited by spin-coating from chloroform solution (12 mg/mL) containing 1.25% volume fraction of 1,8-diiodooctane (DIO) additives. The optimum donor:acceptor (D:A) blend ratio and thickness of BHJ active layer films were found to be 1.3:1 (w/w) and 100−110 nm, respectively. Figure 5 shows the current density−voltage (*J*−*V*) curves obtained for both donor:acceptor polymer blend all-PSCs. The optimized solar cell parameters including short-circuit current density (J_{sc}), the open-circuit voltage (V_{oc}), fill factor (FF), and PCE are summarized in Table 3. The reference polymer P(NDI2OD-T2) is a well-studied acceptor material used with

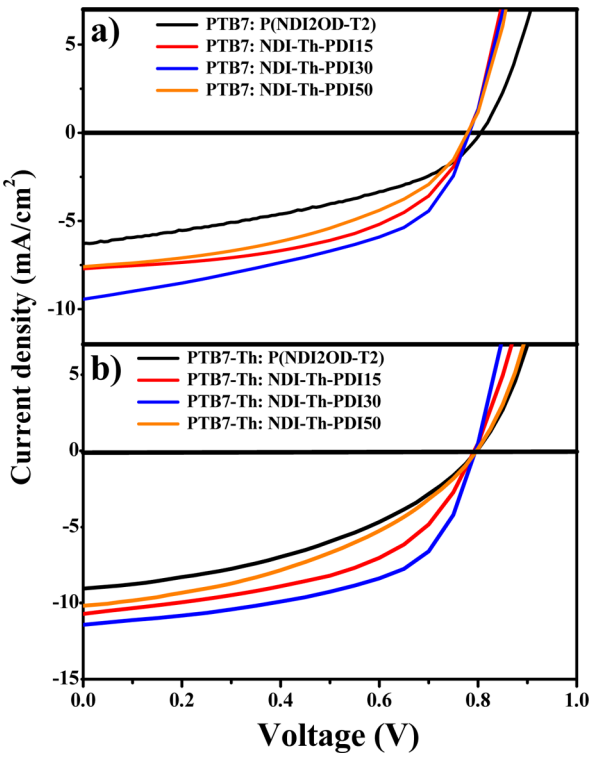

Figure 5. Current density−voltage (*J*−*V*) characteristics for all polymers using (a) PTB7 as the donor and (b) PTB7-Th as the donor.

various low-band-gap polymer and small molecule donors in all-polymer solar cells. In our study, using PTB7 as the donor material, P(NDI2OD-T2) exhibited maximum PCE of 2.06% (J_{sc} of 6.26 mA/cm^2, V_{oc} of 0.81 V, and FF of 40.5%) in device based on the PTB7:P(NDI2OD-T2) blend, and a maximum PCE of 2.97% was obtained (J_{sc} of 9.05 mA/cm^2, V_{oc} of 0.797 V, and FF of 41.3%) using PTB7-Th as the donor material; this optimized PCE is comparable with the previously reported values.[16,21,30,45−47] The device performance of the various PTB7/PTB7-Th:NDI-Th-PDI*x* blend devices showed that all the newly synthesized random copolymers (NDI-Th-PDI15, NDI-Th-PDI30, and NDI-Th-PDI50) exhibited significant improvement in the PCE as compared to reference polymer P(NDI2OD-T2). For instance, PTB7:NDI-Th-PDI15 blend device showed PCE of 3.15% (J_{sc} of 7.71 mA/cm^2, V_{oc} of 0.78, and FF of 52.3%). Further enhancement in the photovoltaic performance was observed in PTB7:NDI-Th-PDI30 blend device which exhibited PCE of 3.56% (J_{sc} of 9.45 mA/cm^2, V_{oc} of 0.78, and FF of 48.0%). However, the PTB7:NDI-Th-PDI50 blend with highest incorporation of PDI (50%) showed lower PCE of 2.72% (J_{sc} of 7.60 mA/cm^2, V_{oc} of 0.77, and FF of 45.9%), which was still higher compared to the reference polymer P(NDI2OD-T2). A similar trend of enhanced photovoltaic performance was observed for blend devices of the random copolymers with PTB7-Th as the donor. The PCE values obtained were 4.22%, 5.03%, and 3.33% for PTB7-Th:NDI-Th-PDI15, PTB7-Th:NDI-Th-PDI30, and PTB7-Th:NDI-Th-PDI50 blend devices, respectively. The dependence of the PCE on the varying incorporation of PDI unit in the copolymer is shown in Figure 6. From Figure 6 it could be observed that NDI-Th-PDI30 reflected the best optimized composition with both donor polymers, and further increase in PDI incorporation into (NDI-Th-PDI*x*) random copolymer did not result in improvement of the photovoltaic performance. The improved device performance upon using PTB7-Th as donor instead of PTB7 in the blend devices with the random copolymers was expected since PTB7-Th had shown face-on molecular orientation and superior photovoltaic properties with various electron acceptor materials.[41] The enhancement in the PCE values of random copolymers NDI-Th-PDI*x* based all-PSCs devices was mainly due to the increase in the J_{sc} value. Additionally, the observed variations in the J_{sc} values with different copolymer compositions were well-reflected in the changes of their spectral response in EQE spectrum, which is shown in Figure 7. All random copolymer blend PTB7:NDI-Th-PDI*x* devices exhibited broad photoresponse in the region of 300−800 nm with higher photocurrent generation compared to reference polymer P(NDI2OD-T2). Particularly, NDI-Th-PDI30 showed highest EQE of 48% at ~605 nm for blend device with PTB7 and 55% at ~615 nm for blend device with PTB7-Th, which was consistent with the observed J_{sc} value (within 2%). A careful observation of EQE spectra revealed the presence of an additional broad peak at ~480 nm for all random copolymers (shown by arrow in Figure 7) that was also observed in their absorption spectra, which was attributed to PDI unit. Thus, the observed EQE spectra showed that the acceptor polymer in blend also contributed to light harvesting and in photocurrent generation.

Bulk Carrier Charge Transport in BHJ Blend Film. The effect of charge carrier transport properties on the photovoltaic performance was investigated by measuring the bulk electron and hole mobility of polymer/polymer blend films using the space-charge-limited current (SCLC) technique. Mobility

DOI: 10.1021/acs.macromol.6b01566
Macromolecules 2016, 49, 8113−8125

Table 3. Photovoltaic Properties of PTB7/PTB7-Th: NDI-Th-PDI*x* and PTB7/PTB7-Th: P(NDI2OD-T2) Blend All-Polymer Solar Cells

active layer	V_{oc} (V)	J_{sc} (mA/cm^2)	FF (%)	PCE (%)
		PTB7 donor		
PTB7:P(NDI2OD-T2)	0.807 ± 0.05	6.19 ± 0.07	40.1 ± 0.04	2.00 ± 0.06
PTB7:NDI-Th-PDI15	0.777 ± 0.03	7.66 ± 0.05	52.1 ± 0.02	3.10 ± 0.05
PTB7:NDI-Th-PDI30	0.780 ± 0.02	9.41 ± 0.04	47.8 ± 0.02	3.50 ± 0.06
PTB7:NDI-Th-PDI50	0.774 ± 0.05	7.55 ± 0.05	45.5 ± 0.04	2.65 ± 0.07
		PTB7-Th donor		
PTB7-Th:P(NDI2OD-T2)	0.793 ± 0.04	8.96 ± 0.09	41.0 ± 0.03	2.91 ± 0.06
PTB7-Th:NDI-Th-PDI15	0.787 ± 0.05	10.65 ± 0.06	49.3 ± 0.04	4.13 ± 0.09
PTB7-Th:NDI-Th-PDI30	0.792 ± 0.03	11.39 ± 0.04	55.2 ± 0.02	4.98 ± 0.05
PTB7-Th:NDI-Th-PDI50	0.793 ± 0.04	10.10 ± 0.06	40.7 ± 0.05	3.26 ± 0.07

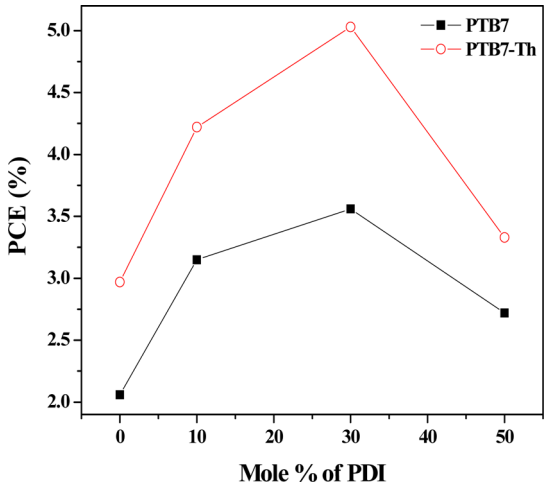

Figure 6. Dependence of PCE on random copolymer composition.

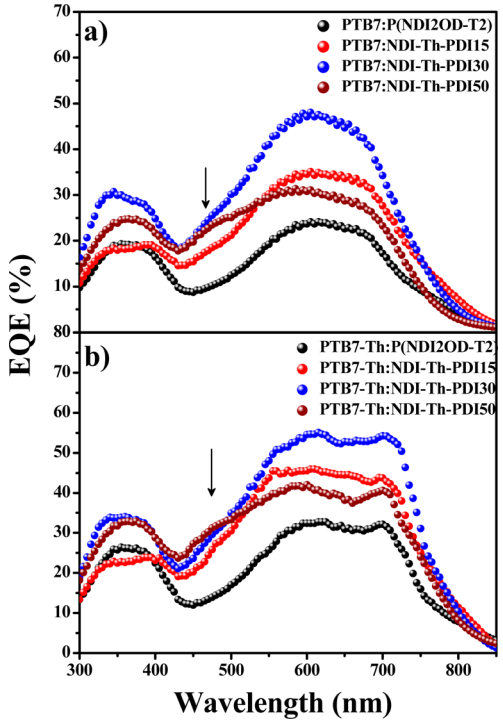

Figure 7. EQE spectra of all-PSCs using (a) PTB7 as the donor and (b) PTB7-Th as the donor in the blend polymer devices (under AM1.5G 100 mW/cm^2 illumination).

measured by the SCLC method is more relevant to the bulk process, e.g., organic photovoltaic device and OLED (organic light-emitting device) devices.[48,49] All donor:acceptor polymer blend film devices were made similarly as the all-PSCs devices. The electron-only device was fabricated using ITO/ZnO/active layer/Al structure, and hole-only device was fabricated using ITO/MoOx/active layer/Au structure (the detailed procedure of device fabrication is given in the Experimental Section). The electron and hole mobility along with (μ_h/μ_e) values obtained from PTB7:acceptor and PTB7-Th:acceptor polymer blend devices are summarized in Table 4, and their *J*−*V* curves with the SCLC fittings are shown in Figure S16. The reference PTB7:P(NDI2OD-T2) blend device exhibited the hole and electron mobility of 6.7 × 10^{-5} and 7.5 × 10^{-5} cm^2/(V s), respectively, while the values of mobilities with PTB7-Th as the donor were (μ_h = 0.9 × 10^{-4} cm^2/(V s) and μ_e = 0.7 × 10^{-4} cm^2/(V s)). Improvements were observed in the hole mobility values for the copolymer blend compositions with higher PDI content, i.e., NDI-Th-PDI30 and NDI-Th-PDI50 with PTB7 (μ_h = 3.8 × 10^{-4} and 3.5 × 10^{-4} cm^2/(V s), respectively), while the electron mobilities values were very similar for all copolymer composition blends. The hole and electron mobility values of the random copolymer blends with PTB7-Th as the donor were of the same order as that of the reference polymer. Among the random copolymers, NDI-Th-PDI30 showed better bulk mobility values (hole and electron) with PTB7 or PTB7-Th blend compositions.

BHJ Solar Cell Morphology. Among various other parameters, the BHJ morphology of active layer (D/A) is one of the important factor that influences the photovoltaic performance.[50] AFM images of donor:acceptor polymer blends were captured to investigate the surface morphology all-PSCs BHJ devices. The donor:acceptor polymer (1.3:1 w/w) blend films were prepared in identical ways as that for all-PSCs devices. Figures S17 and S18 shows AFM height images (3 μm × 3 μm) of PTB7/PTB7-Th:P(NDI2OD-T2) and PTB7/PTB7-Th:NDI-Th-PDI*x* blend solar cells. The reference PTB7:P(NDI2OD-T2) or PTB7-Th:P(NDI2OD-T2) blend films showed rather coarsened morphology with average root-mean-square (RMS) surface roughness of 2.06 and 1.87 nm, respectively, due to the formation of large polymer aggregate domains. The large phase-separated granular morphology observed in PTB7/PTB7-Th:P(NDI2OD-T2) blend film indicated insufficient donor/acceptor intermixing at nanometer scale.[18−42] The incorporation of large PDI unit in the random copolymer showed dramatic change in the surface morphology of PTB7/PTB7-Th:NDI-Th-PDI*x* blend films compared to reference blend. The PTB7:NDI-Th-PDI15 and PTB7:NDI-

DOI: 10.1021/acs.macromol.6b01566
Macromolecules 2016, 49, 8113−8125

Table 4. SCLC Electron and Hole Mobilities of Donor:Acceptor Copolymer Blend[a]

active layer	μ_h ($cm^2/(V\ s)$)	μ_e ($cm^2/(V\ s)$)	μ_h/μ_e
PTB7 donor			
PTB7:P(NDI2OD-T2)	$(6.7 \pm 0.4) \times 10^{-5}$	$(7.5 \pm 0.5) \times 10^{-5}$	0.89
PTB7:NDI-Th-PDI15	$(0.8 \pm 0.3) \times 10^{-4}$	$(8.6 \pm 0.4) \times 10^{-5}$	0.93
PTB7:NDI-Th-PDI30	$(3.8 \pm 0.2) \times 10^{-4}$	$(0.8 \pm 0.2) \times 10^{-4}$	4.75
PTB7:NDI-Th-PDI50	$(3.5 \pm 0.3) \times 10^{-4}$	$(7.6 \pm 0.4) \times 10^{-5}$	4.60
PTB7-Th donor			
PTB7-Th:P(NDI2OD-T2)	$(0.9 \pm 0.3) \times 10^{-4}$	$(0.7 \pm 0.4) \times 10^{-4}$	1.28
PTB7-Th:NDI-Th-PDI15	$(2.6 \pm 0.4) \times 10^{-4}$	$(0.9 \pm 0.3) \times 10^{-4}$	2.88
PTB7-Th:NDI-Th-PDI30	$(4.7 \pm 0.5) \times 10^{-4}$	$(1.1 \pm 0.4) \times 10^{-4}$	4.27
PTB7-Th:NDI-Th-PDI50	$(4.0 \pm 0.4) \times 10^{-4}$	$(1.1 \pm 0.3) \times 10^{-4}$	3.63

[a]In one series PTB-7 was the donor while in the second series PTB7-Th was used as donor.

Th-PDI30 blend films showed proper uniform microphase separation with smaller phase-separated domain size. Furthermore, the RMS surface roughness decreased to 1.08 nm in PTB7:NDI-Th-PDI15 blend and 1.22 nm in the PTB7:NDI-Th-PDI30 blend, which suggested the formation of less aggregated domain leading to better donor/acceptor intermixing at the nanometer scale. The well-developed nanoscale interpenetrating network observed in PTB7:NDI-Th-PDI15 and PTB7:NDI-Th-PDI30 blend films is beneficial for exciton dissociation and charge carrier transport.[51] Compared to the other two random copolymer blend, the PTB7:NDI-Th-PDI50 blend film showed high RMS surface roughness of 1.42 nm with coarsened morphology, which was still more uniform with smaller phase-separated domain size compared to the reference PTB7:P(NDI2OD-T2) blend. A similar trend was observed in the blend films with PTB7-Th as the donor (Figure S18). PTB7-Th:NDI-Th-PDI15 blend and PTB7-Th:NDI-Th-PDI30 blend films showed more uniform mircophase separation (as indicated by the reduced RMS surface roughness) compared to the reference polymer blend. The reduced roughness can play an important role in the charge collection process as it decreases surface recombination and increases the current density as observed from the $J-V$ curves.

CONCLUSIONS

In this study, we report the synthesis of a series of new n-type semiconducting random copolymers NDI-bithiophene/PDI-bithiophene (NDI-Th-PDIx) by incorporating various amounts of perylene diimide (PDI) (xPDI = 15, 30, and 50 mol % of PDI) coacceptor unit into the P(NDI2OD-T2) polymer. The properties of these acceptor copolymers were investigated in depth in the pristine form as well as their donor−acceptor (D:A) blends with PTB7-Th as donor in order to understand the structural features that influence the all-PSCs performance. Proton NMR, XRD, and DSC studies of pristine copolymers showed that increasing PDI content in the random copolymers resulted in progressive reduction of self-aggregation tendency, increased $\pi-\pi$ stacking distance, and lowering of crystallinity. Although the copolymer with lowest PDI content (NDI-Th-PDI 15) exhibited higher ΔH_m compared to P(NDI2OD-T2), its D:A blend with PTB7-Th showed reduced crystallinity compared to PTB7-Th:P(NDI2OD-T2) blend. Analysis of blend properties of these acceptor copolymers with PTB7-Th gave important findings such as: (1) Overall reduction of crystallinity in blends was observed as evidenced by their much lower ΔH_m values compared to the pristine samples. (2) All random copolymers exhibited lower extent of crystallinity compared to P(NDI2OD-T2), and the crystallinity was found to decrease as PDI content increased. (3) XRD of the blend films showed disappearance of the higher ordered lamellar peaks in the random copolymers; the reference polymer seemed to retain them in the blend as well. (4) Higher PL quenching was observed in random copolymer blends as compared to P(NDI2OD-T2). Overall, the random copolymers showed reduced interchain interaction promoting better compatibility with the donor polymer compared to P-(NDI2OD-T2). This was reflected in their bulk photovoltaic properties as well with the random copolymers exhibiting higher PCE compared to P(NDI2OD-T2). A maximum PCE of ∼5% was observed in the case of PTB7-Th:NDI-Th-PDI30 blend devices. A precise correlation of the structural variation among the random copolymers with their device performance was not very straightforward. For instance, although least self-aggregation was observed in NDI-Th-PDI50, it did not exhibit the highest PCE value among the random copolymers. AFM imaging analysis indicated large surface roughness for this blend combination. A probable reason for this discrepancy could be the comparatively low molecular weight of the NDI-Th-PDI50, which was the lowest due to the reduced solubility of the short ethylhexyl side chain on the PDI unit. Our studies showed that presumably NDI-Th-PDI30 exhibited optimal crystallinity and miscibility with donor polymer which led to the best D/A compatibility, nanoscale phase separation, and improved bulk carrier charge transport in the blend. Thus, it is evident from the structure−property analysis that the incorporation of n-type PDI building block into P(NDI2OD-T2) polymer is a very effective strategy to tune its photovoltaic parameters, and improved PCE observed in new n-type random copolymers proves its potential application in future all-PSCs.

ASSOCIATED CONTENT

Supporting Information

The Supporting Information is available free of charge on the ACS Publications website at DOI: 10.1021/acs.macromol.6b01566.

Synthesis of the NDI and PDI monomers, their structural characterization using MALDI-TOF, ^{1}H NMR, GPC, TGA, CV, XRD, AFM, PL, and SCLC curves for the polymers (PDF)

AUTHOR INFORMATION

Corresponding Authors

*(V.G.) E-mail drvinaygupta@netscape.net.
*(S.K.A.) E-mail sk.asha@ncl.res.in.

DOI: 10.1021/acs.macromol.6b01566
Macromolecules 2016, 49, 8113−8125

Author Contributions

S.S. and N.B.K. made equal contributions.

Notes

The authors declare no competing financial interest.

■ ACKNOWLEDGMENTS

This work is financially supported by CSIR network project (TAPSUN) NWP0054. N.B.K. thanks CSIR for a SRF fellowship. S.S. and R.D. thank UGC for a SRF and JRF fellowship, respectively.

■ REFERENCES

(1) Lu, L.; Zheng, T.; Wu, Q.; Schneider, A. M.; Zhao, D.; Yu, L. Recent Advances in Bulk Heterojunction Polymer Solar Cells. *Chem. Rev.* **2015**, *115*, 12666−12731.

(2) Kolhe, N. B.; Shinde, S.; Saibal, B.; Asha, S. K. Novel Approaches in the Design of Donor-Acceptor Oligomeric and Polymeric Materials for Photovoltaic Applications: D/A Blend versus Self-Assembly of D/A by Covalent or Non-Covalent Interaction. *Org. Photonics Photovolt.* **2015**, *3*, 71−100.

(3) Cheng, Y.-J.; Yang, S.-H.; Hsu, C.-S. Synthesis of Conjugated Polymers for Organic Solar Cell Applications. *Chem. Rev.* **2009**, *109*, 5868−5923.

(4) Facchetti, A. Polymer Donor−Polymer Acceptor (all-Polymer) Solar Cells. *Mater. Today* **2013**, *16*, 123−132.

(5) Günes, S.; Neugebauer, H.; Sariciftci, N. S. Conjugated Polymer-Based Organic Solar Cells. *Chem. Rev.* **2007**, *107*, 1324−1338.

(6) Wienk, M. M.; Kroon, J. M.; Verhees, W. J. H.; Knol, J.; Hummelen, J. C.; van Hal, P. A.; Janssen, R. A. J. Efficient Methano[70]fullerene/MDMO-PPV Bulk Heterojunction Photovoltaic Cells. *Angew. Chem., Int. Ed.* **2003**, *42*, 3371−3375.

(7) Vandenbergh, J.; Conings, B.; Bertho, S.; Kesters, J.; Spoltore, D.; Esiner, S.; Zhao, J.; Van Assche, G.; Wienk, M. M.; Maes, W.; et al. Thermal Stability of Poly[2-Methoxy-5-(2′-Phenylethoxy)-1,4-Phenylenevinylene] (MPE-PPV):Fullerene Bulk Heterojunction Solar Cells. *Macromolecules* **2011**, *44*, 8470−8478.

(8) Sivula, K.; Luscombe, C. K.; Thompson, B. C.; Fréchet, J. M. J. Enhancing the Thermal Stability of Polythiophene:Fullerene Solar Cells by Decreasing Effective Polymer Regioregularity. *J. Am. Chem. Soc.* **2006**, *128*, 13988−13989.

(9) Richards, J. J.; Rice, A. H.; Nelson, R. D.; Kim, F. S.; Jenekhe, S. A.; Luscombe, C. K.; Pozzo, D. C. Modification of PCBM Crystallization via Incorporation of C_{60} in Polymer/Fullerene Solar Cells. *Adv. Funct. Mater.* **2013**, *23*, 514−522.

(10) Jung, I. H.; Lo, W.-Y.; Jang, J.; Chen, W.; Zhao, D.; Landry, E. S.; Lu, L.; Talapin, D. V.; Yu, L. Synthesis and Search for Design Principles of New Electron Accepting Polymers for All-Polymer Solar Cells. *Chem. Mater.* **2014**, *26*, 3450−3459.

(11) Li, H.; Hwang, Y.-J.; Earmme, T.; Huber, R. C.; Courtright, B. A. E.; O'Brien, C.; Tolbert, S. H.; Jenekhe, S. A. Polymer/Polymer Blend Solar Cells Using Tetraazabenzodifluoranthene Diimide Conjugated Polymers as Electron Acceptors. *Macromolecules* **2015**, *48*, 1759−1766.

(12) Zhan, X.; Facchetti, A.; Barlow, S.; Marks, T. J.; Ratner, M. A.; Wasielewski, M. R.; Marder, S. R. Rylene and Related Diimides for Organic Electronics. *Adv. Mater.* **2011**, *23*, 268−284.

(13) Würthner, F.; Stolte, M. Naphthalene and Perylene Diimides for Organic Transistors. *Chem. Commun.* **2011**, *47*, 5109.

(14) Guo, X.; Facchetti, A.; Marks, T. J. Imide- and Amide-Functionalized Polymer Semiconductors. *Chem. Rev.* **2014**, *114*, 8943−9021.

(15) Yan, H.; Chen, Z.; Zheng, Y.; Newman, C.; Quinn, J. R.; Dötz, F.; Kastler, M.; Facchetti, A. A High-Mobility Electron-Transporting Polymer for Printed Transistors. *Nature* **2009**, *457*, 679−686.

(16) Kang, H.; Kim, K.-H.; Choi, J.; Lee, C.; Kim, B. J. High-Performance All-Polymer Solar Cells Based on Face-On Stacked Polymer Blends with Low Interfacial Tension. *ACS Macro Lett.* **2014**, *3*, 1009−1014.

(17) Jung, J. W.; Jo, J. W.; Chueh, C.-C.; Liu, F.; Jo, W. H.; Russell, T. P.; Jen, A. K.-Y. Fluoro-Substituted N-Type Conjugated Polymers for Additive-Free All-Polymer Bulk Heterojunction Solar Cells with High Power Conversion Efficiency of 6.71%. *Adv. Mater.* **2015**, *27*, 3310−3317.

(18) Hwang, Y.-J.; Earmme, T.; Courtright, B. A. E.; Eberle, F. N.; Jenekhe, S. A. N-Type Semiconducting Naphthalene Diimide-Perylene Diimide Copolymers: Controlling Crystallinity, Blend Morphology, and Compatibility Toward High-Performance All-Polymer Solar Cells. *J. Am. Chem. Soc.* **2015**, *137*, 4424−4434.

(19) Kim, Y.; Long, D. X.; Lee, J.; Kim, G.; Shin, T. J.; Nam, K.-W.; Noh, Y.-Y.; Yang, C. A Balanced Face-On to Edge-On Texture Ratio in Naphthalene Diimide-Based Polymers with Hybrid Siloxane Chains Directs Highly Efficient Electron Transport. *Macromolecules* **2015**, *48*, 5179−5187.

(20) Kang, H.; Uddin, M. A.; Lee, C.; Kim, K.-H.; Nguyen, T. L.; Lee, W.; Li, Y.; Wang, C.; Woo, H. Y.; Kim, B. J. Determining the Role of Polymer Molecular Weight for High-Performance All-Polymer Solar Cells: Its Effect on Polymer Aggregation and Phase Separation. *J. Am. Chem. Soc.* **2015**, *137*, 2359−2365.

(21) Mori, D.; Benten, H.; Okada, I.; Ohkita, H.; Ito, S. Low-Bandgap Donor/Acceptor Polymer Blend Solar Cells with Efficiency Exceeding 4%. *Adv. Energy Mater.* **2014**, *4*, 1301006.

(22) Hwang, Y.-J.; Courtright, B. A. E.; Ferreira, A. S.; Tolbert, S. H.; Jenekhe, S. A. 7.7% Efficient All-Polymer Solar Cells. *Adv. Mater.* **2015**, *27*, 4578−4584.

(23) Earmme, T.; Hwang, Y.-J.; Murari, N. M.; Subramaniyan, S.; Jenekhe, S. A. All-Polymer Solar Cells with 3.3% Efficiency Based on Naphthalene Diimide-Selenophene Copolymer Acceptor. *J. Am. Chem. Soc.* **2013**, *135*, 14960−14963.

(24) Kim, R.; Amegadze, P. S. K.; Kang, I.; Yun, H.-J.; Noh, Y.-Y.; Kwon, S.-K.; Kim, Y.-H. High-Mobility Air-Stable Naphthalene Diimide-Based Copolymer Containing Extended Π-Conjugation for N-Channel Organic Field Effect Transistors. *Adv. Funct. Mater.* **2013**, *23*, 5719−5727.

(25) Hwang, Y.-J.; Murari, N. M.; Jenekhe, S. A. New N-Type Polymer Semiconductors Based on Naphthalene Diimide and Selenophene Derivatives for Organic Field-Effect Transistors. *Polym. Chem.* **2013**, *4*, 3187.

(26) Hwang, Y.-J.; Earmme, T.; Subramaniyan, S.; Jenekhe, S. A. Side Chain Engineering of N-Type Conjugated Polymer Enhances Photocurrent and Efficiency of All-Polymer Solar Cells. *Chem. Commun.* **2014**, *50*, 10801.

(27) Chen, Z.; Zheng, Y.; Yan, H.; Facchetti, A. Naphthalenedicarboximide- vs Perylenedicarboximide-Based Copolymers. Synthesis and Semiconducting Properties in Bottom-Gate N-Channel Organic Transistors. *J. Am. Chem. Soc.* **2009**, *131*, 8−9.

(28) Steyrleuthner, R.; Schubert, M.; Howard, I.; Klaumünzer, B.; Schilling, K.; Chen, Z.; Saalfrank, P.; Laquai, F.; Facchetti, A.; Neher, D. Aggregation in a High-Mobility N-Type Low-Bandgap Copolymer with Implications on Semicrystalline Morphology. *J. Am. Chem. Soc.* **2012**, *134*, 18303−18317.

(29) Fabiano, S.; Chen, Z.; Vahedi, S.; Facchetti, A.; Pignataro, B.; Loi, M. A. Role of Photoactive Layer Morphology in High Fill Factor All-Polymer Bulk Heterojunction Solar Cells. *J. Mater. Chem.* **2011**, *21*, 5891.

(30) Moore, J. R.; Seifried, S. A.; Rao, A.; Massip, S.; Watts, B.; Morgan, D. J.; Friend, R. H.; McNeill, C. R.; Sirringhaus, H. Polymer Blend Solar Cells Based on a High-Mobility Naphthalenediimide-Based Polymer Acceptor: Device Physics, Photophysics and Morphology. *Adv. Energy Mater.* **2011**, *1*, 230−240.

(31) Schubert, M.; Dolfen, D.; Frisch, J.; Roland, S.; Steyrleuthner, R.; Stiller, B.; Chen, Z.; Scherf, U.; Koch, N.; Facchetti, A. Influence of Aggregation on the Performance of All-Polymer Solar Cells Containing Low-Bandgap Naphthalenediimide Copolymers. *Adv. Energy Mater.* **2012**, *2*, 369−380.

DOI: 10.1021/acs.macromol.6b01566
Macromolecules 2016, 49, 8113−8125

(32) Li, Z.; Xu, X.; Zhang, W.; Meng, X.; Ma, W.; Yartsev, A.; Inganäs, O.; Andersson, M. R.; Janssen, R. A. J.; Wang, E. High Performance All-Polymer Solar Cells by Synergistic Effects of Fine-Tuned Crystallinity and Solvent Annealing. *J. Am. Chem. Soc.* **2016**, *138*, 10935−10944.
(33) Kim, Y.; Cho, H.-H.; Kim, T.; Liao, K.; Kim, B. Terpolymer approach for controlling the crystalline behavior of naphthalene diimide-based polymeracceptors and enhancing the performance of all-polymer solar cells. *Polym. J.* **2016**, *48*, 517−524.
(34) Li, X.; Sun, P.; Wang, Y.; Shan, H.; Xu, J.; You, C.; Xu, Z.-X.; Chen, Z.-K. Design of three-component randomly incorporated copolymers as non-fullerene acceptors for all-polymer solar cells. *Polym. Chem.* **2016**, *7*, 2230−2238.
(35) Dai, S.; Cheng, P.; Lin, Y.; Wang, Y.; Ma, L.; Ling, Q.; Zhan, X. Perylene and Naphthalene Diimide Polymers for All-Polymer Solar Cells: A Comparative Study of Chemical Copolymerization and Physical Blend. *Polym. Chem.* **2015**, *6*, 5254−5263.
(36) Kozycz, L. M.; Gao, D.; Tilley, A. J.; Seferos, D. S. One Donor−Two Acceptor (D−A1)-(D−A2) Random Terpolymers Containing Perylene Diimide, Naphthalene Diimide, and Carbazole Units. *J. Polym. Sci., Part A: Polym. Chem.* **2014**, *52*, 3337−3345.
(37) Mott, N. F.; Gurney, R. W. *Electronic Processes in Ionic Crystals*; Oxford University Press: London, 1940.
(38) Jones, B. A.; Ahrens, M. J.; Yoon, M.-H.; Facchetti, A.; Marks, T. J.; Wasielewski, M. R. High-Mobility Air-Stable N-Type Semiconductors with Processing Versatility: Dicyanoperylene-3,4:9,10-Bis(dicarboximides). *Angew. Chem., Int. Ed.* **2004**, *43*, 6363−6366.
(39) Popere, B. C.; Della Pelle, A. M.; Thayumanavan, S. BODIPY-Based Donor−Acceptor Π- Conjugated Alternating Copolymers. *Macromolecules* **2011**, *44*, 4767−4776.
(40) Kolhe, N. B.; Ashar, A. Z.; Narayan, K. S.; Asha, S. K. Naphthalene Diimide Copolymers with Oligo(*p* -Phenylenevinylene) and Benzobisoxazole for Balanced Ambipolar Charge Transport. *Macromolecules* **2014**, *47*, 2296−2305.
(41) Jung, J.; Lee, W.; Lee, C.; Ahn, H.; Kim, B. J. Controlling Molecular Orientation of Naphthalenediimide-Based Polymer Acceptors for High Performance All-Polymer Solar Cells. *Adv. Energy Mater.* **2016**, *6*, 1600504.
(42) Schuettfort, T.; Huettner, S.; Lilliu, S.; Macdonald, J. E.; Thomsen, L.; McNeill, C. R. Surface and Bulk Structural Characterization of a High-Mobility Electron-Transporting Polymer. *Macromolecules* **2011**, *44*, 1530−1539.
(43) Lee, W.; Lee, C.; Yu, H.; Kim, D.-J.; Wang, C.; Woo, H. Y.; Oh, J. H.; Kim, B. J. Side Chain Optimization of Naphthalenediimide-Bithiophene-Based Polymers to Enhance the Electron Mobility and the Performance in All-Polymer Solar Cells. *Adv. Funct. Mater.* **2016**, *26*, 1543−553.
(44) Durban, M. M.; Kazarinoff, P. D.; Luscombe, C. K. Synthesis and Characterization of Thiophene-Containing Naphthalene Diimide N-Type Copolymers for OFET Applications. *Macromolecules* **2010**, *43*, 6348−6352.
(45) Jung, J. W.; Russell, T. P.; Jo, W. H. A Small Molecule Composed of Dithienopyran and Diketopyrrolopyrrole as Versatile Electron Donor Compatible with Both Fullerene and Nonfullerene Electron Acceptors for High Performance Organic Solar Cells. *Chem. Mater.* **2015**, *27*, 4865−4870.
(46) Zhou, N.; Lin, H.; Lou, S. J.; Xinge, Y.; Guo, P.; Manley, E. F.; Loser, S.; Hartnett, P.; Huang, H.; Wasielewski, M. R.; Chen, L. X.; Chang, R. P. H.; Facchetti, A.; Marks, T. J. Morphology-Performance Relationships in High-Efficiency All-Polymer Solar Cells. *Adv. Energy Mater.* **2014**, *4*, 1300785.
(47) Mori, D.; Benten, H.; Okada, I.; Ohkita, H.; Ito, S. Highly efficient charge-carrier generation and collection in polymer/polymer blend solar cells with a power conversion efficiency of 5.7%. *Energy Environ. Sci.* **2014**, *7*, 2939−2943.
(48) Steyrleuthner, R.; Schubert, M.; Jaiser, F.; Blakesley, J. C.; Chen, Z.; Facchetti, A.; Neher, D. Bulk Electron Transport and Charge Injection in a High Mobility n-Type Semiconducting Polymer. *Adv. Mater.* **2010**, *22*, 2799−2803.
(49) Rivnay, J.; Steyrleuthner, R.; Jimison, L. H.; Casadei, A.; Chen, Z.; Toney, M. F.; Facchetti, A.; Neher, D.; Salleo, A. Drastic Control of Texture in a High Performance n-Type PolymericSemiconductor and Implications for Charge Transport. *Macromolecules* **2011**, *44*, 5246−5255.
(50) Zhou, N.; Lin, H.; Lou, S. J.; Xinge, Y.; Guo, P.; Manley, E. F.; Loser, S.; Hartnett, P.; Huang, H.; Wasielewski, M. R.; Chen, L. X.; Chang, R. P. H.; Facchetti, A.; Marks, T. J. Morphology-Performance Relationships in High-Efficiency All-Polymer Solar Cells. *Adv. Energy Mater.* **2014**, *4*, 1300785.
(51) Huang, Y.; Kramer, E. J.; Heeger, A. J.; Bazan, G. C. Bulk Heterojunction Solar Cells: Morphology and Performance Relationships. *Chem. Rev.* **2014**, *114*, 7006−7043.

DOI: 10.1021/acs.macromol.6b01566
Macromolecules 2016, 49, 8113−8125